Deformation Behavior of Fe-3%Si Steel at High Temperatures

R. Kaibyshev and I. Kazakulov

Institute for Metals Superplasticity Problems RAS, RU-450001, Khalturina 39, Ufa, Russia

Keywords: Deformation, Threshold Behavior, Activation Energy, Threshold Stress

Abstract

Deformation behavior of a Fe-3%Si steel with ultrafine MnS inhibitors was studied in the temperature range 500-1000°C. The steel exhibits a threshold behavior. Analysis in terms of threshold stress shown that there were two characteristic modes of deformation behavior in the power-law creep regime. At temperatures 500-700°C the value of the stress exponent, n, is equal to 6, and the true activation energy for plastic deformation, Q, linearly increases from 170 kJ/mol to value closed to 239 kJ/mol with temperature rise. At temperatures above 700°C the stress exponent is about 4, and the true activation energy for plastic deformation is about 240 kJ/mol. Two temperature dependencies of normalized threshold stress differed by a value of the energy term, Q_o, were found in these two temperature intervals. The value Q_o is about 55 and 39 kJ/mol in an intermediate and high temperature range, respectively. Operating deformation mechanisms in two temperature regions are discussed.

1. Introduction

The raise of service temperature is very important for some alloys and steels used at high temperatures. Dispersion strengthening is an attractive approach to enhance the creep resistance of these materials due to introducing of ultrafine dispersoids into metallic matrix. It leads to appearance of threshold stress and an improvement of creep resistance at high temperatures. In spite of numerous works dealing with creep of dispersion strengthened materials [1-9], their deformation behavior is insufficiently understood [10-11]. The main limitation of existing threshold models is the fact that there is no prediction of the experimentally observed strong temperature dependence of threshold stress. This dependence could not been attributed to the shear modulus temperature dependence [7,9,10]. At present the origin of such strong temperature dependence of threshold stress is not yet clear. It should be noted that reported experimental data of threshold behavior of dispersion strengthened materials were obtained in rather narrow temperature interval. Complex examination of the temperature dependence of threshold stress in a wide temperature range has not been performed yet.

Thus, the aim of the present study is to report threshold behavior of well-known steel Fe-3%Si at high and intermediate temperatures.

2. Experimental material and procedures

The material of testing was a hot-rolled ferritic Fe-3%Si steel supplied by ChMZ, Chelyabinsk, Russia, having the following chemical composition: 3.1%Si, 0.06%Mn, 0.025%S, 0.025%C, 0.06%N, 0.01%P, 0.03%Cr, 0.06%Ni, 0.06Cu, 0.003%Al, 0.008%As, Fe balance. The average matrix grain size was about 5mm. The material contains several types of dispersion particles. MnS inhibitors are dominant precipitations in this type of Fe-3%Si steel. The number of spherical-shaped particles was approximately 1.7×10^{18} particles/m^3 and their average size was about 80nm.

The specimens with 10 mm in diameter and 15mm in height were machined in perpendicular to the prior rolling direction. Compression test was conducted in temperature interval 500-1000°C at strain rates of 10^{-6} to 10^{-2} s^{-1} using testing machine Schenck-RMS100. For surface examinations the specimens were prepolished by a diamond paste and deformed to the strain ε=15% at $\dot{\varepsilon}=7.0\cdot10^{-4}$ s^{-1}. Surface observations of deformed specimens were performed using a SEM JSM-840.

3. Experimental results

3.1 Mechanical properties

3.1.1 The shape of σ-ε curves. Two temperature intervals differed by a shape of true stress-strain curves were found (Fig.1). In temperature range 800-1000°C the plastic flow attains a stable stage after minor strain. At intermediate temperatures, 500-700°C, three stages of plastic deformation are observed. Minor strain hardening takes place at first stage at $\varepsilon\leq15\%$. The strain hardening coefficient, θ, decreases from 0.9-1.0 at $\varepsilon\leq1$-1.5% to 0.6-0.8 MPa/mm^2 with increasing strain. The second stage is a well-established steady-state region. The duration of the secondary stage is essentially short and does not exceed ε=30-35%. Extensive strain hardening occurs at the third stage where strain hardening coefficient increases from 1-2 at ε=35% up to 5-7 MPa/mm^2 at ε=45%.

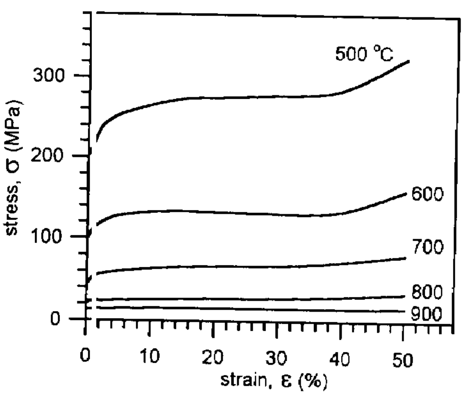

Fig. 1. Typical true stress - strain curves for Fe-3%Si steel in temperature interval 500-900°C at $\dot{\varepsilon}=7.0\cdot10^{-4}$ s^{-1}.

3.1.2 The variation of steady-state stress with strain rate. Figure 2 shows the variation of initial strain rate with flow stress plotted logarithmically. It is seen that deformation behavior of the steel at temperatures above 500°C is described in terms of the power law

$$\dot{\varepsilon} = A\cdot\sigma^{n}\cdot\exp\left(\frac{-Q}{R\cdot T}\right) \qquad (1)$$

where A is a constant, n is the stress exponent, σ is the steady state flow stress, Q is the activation energy for plastic deformation, R is the gas constant and T is the absolute temperature. In temperature range 600-1000°C the values of stress exponent vary from 6 to 7.8 and do not remarkably depend on temperature and strain rate. At temperatures 500-550C the values n increase up to 9-9.3. Notice that at temperatures less than 500°C the power law breakdown takes place.

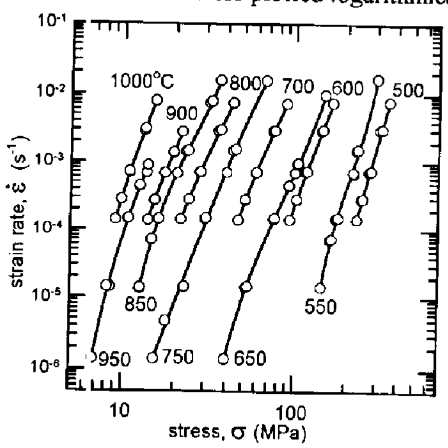

Fig 2. Double logarithmic plot of the initial strain rate *vs* flow stress for temperatures from 500 to 1000°C.

3.1.3 The activation energy for plastic deformation. Algebraically, Eq.1 can be converted [12] to

$$\ln\sigma = \ln(\dot{\varepsilon}/A)^{1/n} + \frac{Q}{Rn}\cdot\frac{1}{T} \quad (2)$$

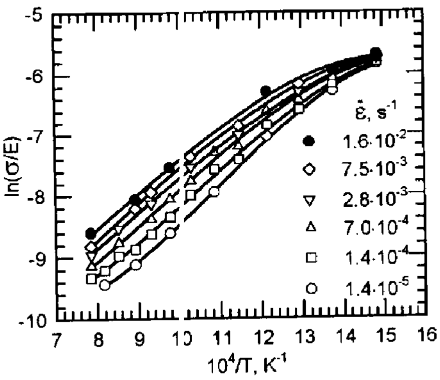

Fig. 3. Elastic modulus-compensated flow stress vs inverse of absolute temperature.

The apparent activation energy for plastic deformation, Q_a, was obtained graphically by logarithmic plotting of the normalized stress compensated by non-linear temperature dependence of the elastic modulus [13], σ/E, against the inverse of the absolute temperatures and taking the slope of tangent to be Q/(Rn) (Fig.3) for different strain rates.

It is seen, that calculated values of Q_a, lying in range from 300 to 400 kJ/mol, are much higher than the activation energy for self-diffusion in α-Fe (Q_f=239 kJ/mol) [13].

3.2 Surface observation

The surface metallographic features were found to be dependent on temperature (Fig.4). At all examined temperatures, the slip morphology observed in this investigation could be classified as multiple slip. Wavy slip features indicate that there is extensive cross slip occurrence. Temperature decrease leads to localization of dislocation glide. At high temperatures uniform dislocation sliding takes place and extensive microscopic strain localization is observed at low temperatures.

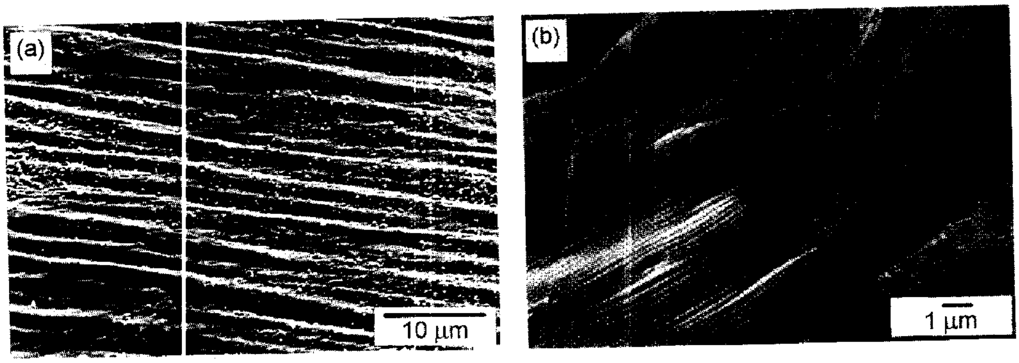

Fig. 4. Deformation relief of Fe-3%Si specimens deformed up to ε=15% at $\dot{\varepsilon}$=7.0·10^{-4} s^{-1}: a) t=600°C; b) t=900°C.

4. Analysis and Discussion

4.1. An examination of threshold stress. It is obvious that deformation behavior of the Fe-3%Si steel cannot be described over a wide examined range of strain rate and temperature by Eq.1. It is known [7-10] that an increase of the stress exponent with decreasing strain rate and the high values of the activation energy for plastic deformation are attributed to threshold behavior of a material. Therefore, the following phenomenological equation for plastic deformation can be used

$$\dot{\varepsilon} = A\cdot\left(\frac{\sigma-\sigma_o}{E}\right)^n\cdot\exp\left(\frac{-Q}{R\cdot T}\right) \quad (3)$$

where σ_o is threshold stress.

The standard procedure was used to determine the threshold stress [7,9,10]. In estimating the threshold stress, σ_o, the experimental data were plotted as $\dot{\varepsilon}^{1/n}$ against σ on a double linear scale (Fig.4) at a temperature in the range t=500-900°C. This graphic method can be used if the deformation of a material obeys equation Eq.3 and if σ_o is independent from the strain rate. The datum points in this strain rate interval fit with excellent accuracy to a straight line by varying the stress exponent, as 3,4,5,6,7 and 8. Extrapolation of this line to zero gives the value σ_o. The obtained values of threshold stress at different temperatures are presented in Table 1.

Table 1. Threshold stress at different temperatures.

t, °C	500	550	600	650	700	750	800	850	900
n	6	6	6	6	5	4	4	4	4
σ_o, MPa	133.0	90.4	34.9	24.7	22.2	12.1	9.0	7.4	6.9

The temperature dependence of normalized threshold stress, σ_o/E, can be represented by [6, 7]

$$\frac{\sigma_o}{E} = B_o \exp\left(\frac{Q_o}{RT}\right) \quad (4)$$

where B_o is a constant, and Q_o is an energy term [9]. The value of Q_o can be obtained graphically by plotting $\ln(\sigma_o/E)$ *vs* 1/T (Fig. 5). It is seen that there are two temperature intervals which differ in a value of energy term. At high temperatures (700-900°C) it is 39kJ/mol and at intermediate temperatures (500-700°C) this value is higher, 55kJ/mol. It should be noted that temperature dependence of threshold stress was reported for classic superplastic materials and for aluminum alloys and metal matrix composites on their base, produced via powder metallurgical techniques [7,9]. However, the temperature influence on the energy term in Eq.4 has not been reported yet. It seems that it was caused by the fact that threshold behavior of numerous materials was examined in the narrow temperature interval which did not exceed 100°C. As a result, the transition from one value of energy term to the other was not found.

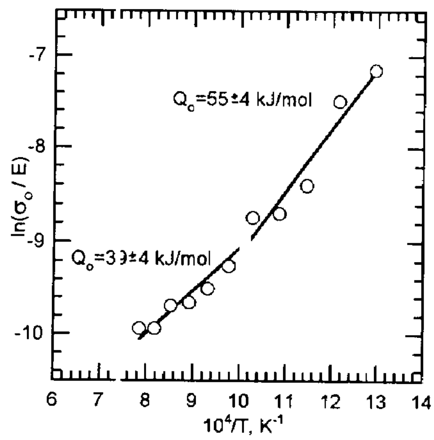

Fig. 5. The temperature dependence of the normalized threshold stress.

It is seen that deformation behavior of the Fe-3%Si steel is typical for behavior of dispersion strengthened alloys. It is caused by the presence of ultrafine MnS inhibitors. It is known [14-16] that there is no remarkable temperature dependence of MnS precipitate size and their volume fraction at t<900°C. Consequently, the transition in threshold behavior of the steel is associated with change of interaction mechanism between dislocations and the hard obstacles.

4.2. An examination of the normalized deformation data. The data of the analysis of deformation behavior of the Fe-3%Si steel in terms of threshold stress (Fig.2, Table 1) allow to plot the normalized strain rate, $\dot{\varepsilon}kT/(D_l E b)$, against the normalized effective stress, $(\sigma-\sigma_o)/E$ (Fig.6). There $D_l = 2\cdot 10^{-4}\exp(-251/(RT))$ is the lattice diffusion coefficient in α-iron.

It is seen that the steel exhibits two characteristic modes of deformation behavior. First, at high temperatures, 700-1000°C, and at low normalized strain rate, $\dot{\varepsilon}kT/(D_l E b)<10^{-8}$, there is a well-defined power-law relationship with n=4.1. Such deformation behavior is associated with dislocation climb controlling by lattice diffusion [17]. This region locates below the Sherby-Burke criterion ($\dot{\varepsilon}kT/(D_l G b)\cong 10^{-8}$) which has to represent the breakdown of the power law. At intermediate temperatures, 500-700°C, the slope of straight line dependence $\dot{\varepsilon}kT/(D_lEb)$ *vs* $(\sigma-\sigma_o)/E$ is equal to 6. Such transition could be interpreted in terms of transition to low temperature climb controlled by pipe-diffusion along the dislocation cores. The classic relationship $n_{it}=n_{ht}+2$ is observed for transition from high to intermediate temperature. Notice, that the experimental points in that region lie above the Sherby-Burke criterion which exactly matches transition from one interval of power-law creep to another. From this point of view there is an unambiguous of such simple interpretation of presented results.

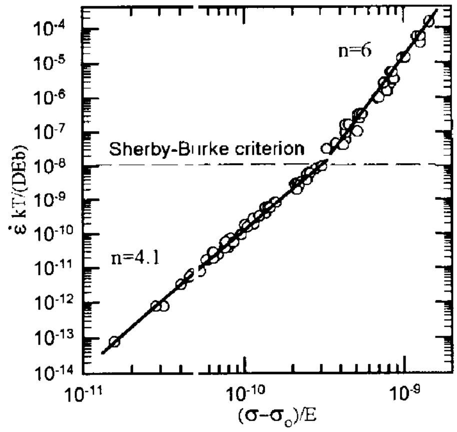

Fig. 6. Normalized strain rate vs normalized stress, showing the transition from power-law plastic deformation with n=4.1 (high temperature region) to the creep with n=6 (intermediate temperature region)

The temperature of transition from one region of the power law to another and the temperature which is the inflection point for threshold behavior of the Fe-3%Si steel are similar. The change of rate-controlling deformation processes is accompanied by change of mechanism of interaction between dispersoids and lattice dislocation. Thus, it is possible to presume that there is a connection between mechanism of interaction between dislocations and obstacles and a rate-controlling mechanism of plastic deformation.

4.3. True activation energy for plastic deformation in two intervals of power-law creep. The true activation energy for plastic deformation, Q, in Eq.3 could be determined, as mentioned above, by logarithmic plotting the elastic modulus compensated effective stress *vs* the inverse absolute temperatures (Fig 7). In addition, we should take into account the existence of non-linear temperature dependence of elastic modulus caused by the second order phase transition in Fe-3%Si

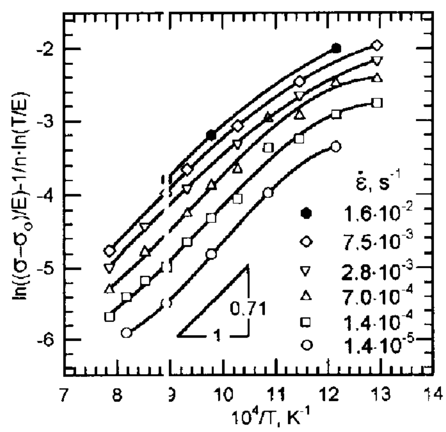

Fig. 7. Normalized effective stress vs inverse of absolute temperature.

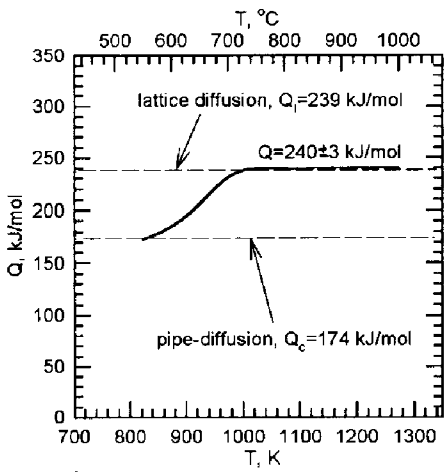

Fig.8. Temperature dependence of the true activation energy.

steel. Therefore the graphical plot $\ln((\sigma-\sigma_o)/E)-1/n\cdot\ln(T/E)$ *vs* 1/T was made. The second term on the ordinate axis is the modulus correction of non-linearity of temperature dependence, in which the value of n was chosen 4.1 in the examined temperature interval. The slopes of the tangent to the curves at t≥700°C are virtually unchanged and are about 7100K. At lower temperatures the value of the slope decreases to 2100-2600K down to 500°C, monotonically.

The true activation energy calculated from the slope Q/(Rn) are presented in Fig.9. Notice that here we used true values of n from Table 1. It is seen that classic temperature dependence [17] of true activation energy is observed. At t≥700°C the value of Q does not change and is 240±3 kJ/mol. It coincides with exellent accuracy with the value of activation energy of lattice self-diffusion in α-iron (Q_l=239 kJ/mol). In temperature interval 500-700°C the true activation energy decreases to 170±10 kJ/mol, approaching asymptotically to activation energy for pipe diffusion, 174 kJ/mol [13].

It may argued from presented results that the transition from one controlling mechanism of plastic deformation to another, with temperature, results in a change of mechanism of an interaction between dislocations and dispersoids. There is a strong connection between the dislocation ability to climb and the dislocation mechanism to surmount an obstacle. At higher temperatures the general dislocation climb is a controlling mechanism of plastic deformation and dislocations overcome obstacles, easily. A decrease of a dislocation climb velocity at intermediate temperatures causes growth of activation term associating with the barrier to dislocation bypass. At present the origin of the temperature dependence is not entirely clear. However, it is obvious that the dependence could not be explained on the base of existing models [1-3,7,12] and new models should be developed.

5. Conclusion

It was shown that deformation behavior of the Fe-3%Si steel at intermediate temperatures 500-700°C and at high temperature 700-1000°C was different.

1. The value of the stress exponent, n, decreases from ~6 at the intermediate temperature to ~4.1 above ~700°C.
2. The true activation energy for deformation, Q, decreases linearly with increasing normalized stress from ~240 kJ/mol at temperatures 700-1000°C to ~170kJ/mol at t=500°C.
3. It is demonstrated that high temperature data having n=4.1 lie below the Sherby-Burke criterion ($\dot{\varepsilon}kT/(D_l G b) \cong 10^{-8}$) and intermediate temperature data having n=n+2 lie above this criterion..
4. Two different temperature dependencies of threshold stress were found. At intermediate temperatures the energy term, Q_o, is ~55 kJ/mol and at high temperature Q_o is equal to ~39 kJ/mol.

6. References

[1] E.Arzt, J.Rösler, Acta Metall. 36 (1988), p.1043.
[2] E.Arzt, J.Rösler, Acta Metall. 36 (1988), p.1052.
[3] E.Arzt, D.S.Wilkinson, Acta Metall. 34 (1986), p.1893.
[4] W.C.Oliver, W.D.Nix, Acta Metall. 30 (1982), p.1335.
[5] R.W.Lund, W.D.Nix, Met. Trans. 6A (1975), p.1329.
[6] K.T.Park, E.Lavernia and F.Mohamed, Acta Metall. 38 (1990), p.2149.
[7] F.A.Mohamed, K.T.Park and E.J.Lavernia, Mater. Sci. Eng. A150 (1992), p.21.
[8] J.Rosler E.Arzt, Acta Metall.Mater., 38 (1990), p.671.
[9] K.T.Park, E.Lavernia and F. Mohamed, Acta Metall. Mater., 42 (1994), p.667.
[10] J.Cadek, H.Oikawa, V.Sustek, Mater. Sci. Eng. A190 (1995), p.9.
[11] F.Dobes, K.Kucharova, A.Orlova, K.Milicka, J.Cadek, Mater. Sci. Eng. A174 (1994), p.37.
[12] J.R.Pickens, T.J.Langan, R.O.England and M.Liebson, Metall. Trans. 18A (1987), p.303.
[13] H.J.Frost, M.F.Asnby, Deformation-mechanism maps, Pergamon Press (1982).
[14] H.E.Grenoble, J. Appl. Phis. 38 (1967), p.1083.
[15] J.W.Flowers, S.P.Karas, J. Appl. Phys. 38 (1967), p.1085.
[16] W.M.Swift, Metall.Trans. 4 (1973), p.153.
[17] S.V.Raj, T.G.Langdon, Acta Metall. 37 (1989), p.843.

For correspondence: Prof. Rustam Kaibyshev, fax: +7 (3472) 253856, e-mail: ilkaz@anrb.ru